EXPERIMENTAL DETERMINATION OF THE EFFECTIVENESS OF A SOUND ABSORBING TURBINE EXIT CASING

M. Zenz[1], F. Schönleitner[1], L.Simonassi[2], S. Bauinger[1], D. Broszat[3], F. Heitmeir[1], and A. Marn[1]

[1] Institute for Thermal Turbomachinery and Machine Dynamics, Graz University of Technology, Graz, Austria

[2] DIMSET-University of Genova, Genoa, Italy

[3] MTU Aero Engines AG, Munich, Germany

ABSTRACT

This work presents results from experimental investigations conducted in the subsonic test turbine facility for aerodynamic, acoustic, and aeroelastic investigations at Graz University of Technology. The experiments have been performed for the acoustically relevant operating point approach under engine relevant conditions. The sound absorbing exit guide vanes of the turbine exit casing have been designed as Helmholtz resonators with a resonance frequency according to the blade passing frequency of an aero design point. In order to prove the effectiveness of that exit guide vanes acoustic measurements and modal decomposition have been performed and the sound power per azimuthal mode was calculated and compared with results of a conventional hard wall exit guide vane of aerodynamic design. It is shown that the sound power level can be reduced significantly by about 23 dB. However, the losses are increased dramatically.

KEYWORDS

SOUND POWER REDUCTION, ACOUSTICS, SOUND ABSORBER, TURBINE EXIT GUIDE VANES, LOW PRESSURE TURBINE

NOMENCLATURE

Abbreviations

BPF	Blade Passing Frequency
CS	Corner Separation
EGV	Exit Guide Vane
FoI	Frequency of Interest
LPT	Low Pressure Turbine
LPV	Lower Passage Vortex
MTF	Mid Turbine Frame
PS	Pressure Side
SS	Suction Side
STTF-AAAI	Subsonic Test Turbine Facility for Aerodynamic, Acoustic, and Aeroelastic Investigations
TEC	Turbine Exit Casing
TEGV	Turbine Exit Guide Vane
UPV	Upper Passage Vortex

Greek

α	Yaw angle, complex factor	ω	Angular frequency
σ	Eigenvalue of the Bessel function	φ	Circumferential coordinate
ζ	Total pressure loss coefficient	δ	End correction factor (form factor)

Symbols

A	Amplitude	p	Pressure
B	Blade count	r	Radius
c	Speed of sound	R	Outer Radius of the annulus
f	Frequency, modal shape factor	S	Resonator holes section
k	Axial wave number	t	Time
l	Resonator neck length	T	Temperature
m	Azimuthal mode order	V	Vane count, Resonator volume
Ma	Mach number	x	Axial distance, axial coordinate
n	Radial mode order		

Subscript

ax	Axial	res	Resonator
c	Cut-Off	s	Scattered
C,D	Measurement Planes C and D	t	Total
m,n	Azimuthal, radial mode order	tot	Total
ref	Reference		

Superscript

±	Propagation in (+) and against (-) flow direction
$\sim$	Area averaged
$\overline{\sim}$	Mass averaged

INTRODUCTION

Aircraft noise is one of the limiting factors in the growth of future air traffic and is further strictly regulated by law. Also, the Advisory Council for Aviation Research and innovation in Europe (ACARE) has published their goals to reduce environmental impact of air transportation. Since then the commercial and political pressure to reduce CO_2, NO_x, and noise (up to 20dB reduction of noise level until 2020 compared to technologies of the year 2000) has been increased considerably. Between the various components contributing to the overall aircraft noise the engine has a large share. However, the rotor of the last stage of the low pressure turbine interacting with the turbine exit casing's (TEC) guide vanes is the major contributor to the overall engine noise during flight operations in the proximity of the ground, i.e. during take-off, side line, and approach manoeuvres.

For state-of-the art design of turbine exit guide vanes (TEGVs) structural requirements are more important than the aerodynamical and/or the acoustical point of view. Today the TEGVs have to support the rear bearing and the engine mount and therefore they are relatively thick and rigid. However, the TEGVs also have to fulfil aerodynamic aspects. Their main aerodynamic purpose is to reduce swirl in the flow. The goal is to generate homogeneous low pressure turbine (LPT) exit flow by transforming swirl into thrust for highest propulsive efficiencies (Koch, et al., 2012). If structural requirements are of minor interest, for example if the rear bearing and the engine mount is moving forward near the mid turbine frame (MTF) supported by the MTF struts, an optimisation of the (turbine) EGVs may lead to a highly efficient low Reynolds number EGV (Schreiber, et al., 2004). However, the EGVs downstream of a last stage LPT have to have a large operating range in order to provide a near axial outflow for all operating points of the turbine.

The number of investigations on modern low Reynolds number turbine exit guide vanes are limited e.g. (Sonoda, et al., 2004), (Sonoda & Schreiber, 2007) and (Hjärne, 2007). (Koch, et al., 2012) investigated a cross section at 33% blade height of the acoustically optimised TEGVs used in this investigation in a linear cascade as a baseline design. They experimentally and numerically showed that an aerodynamically optimised TEGV meets all requirements for an EGV. The turning was similar to the baseline design and for the entire operating range the outlet flow angle was nearly axial. Further (Koch, et al., 2012) achieved a significant loss reduction for the optimised airfoil and a slightly higher pressure rise due to lower losses at reduced wetted surface. (Marn, et al., 2014) showed that a reduction of 5dB in sound power level is possible by applying an inverse cut-off design, however the losses increased significantly for the off design point approach. (Broszat, et al., 2012) verified this effect numerically and compared it with experimental results. (Marn, et al., 2015) showed the increase of the sound power level for an aerodynamically optimised TEC when compared to a state-of-the-art TEGV. (Marn, et al., 2016) showed that the rotor-TEC interaction is a major contributor to the overall sound power emanated from the engine and that it is worth to put a lot of effort into techniques to reduce that noise component. However, that work was focused on the first blade passing frequency (BPF). All that publications show that the noise generated by rotor-TEC interaction at the operating point approach can be reduced and must be reduced in order to support the goal to achieve the ACARE 2020 targets.

This paper demonstrates the effectiveness of a Helmholtz resonator TEGV under engine realistic operating conditions. The present work reduces the amplitude of the sound pressure at a distinct frequency of interest.

EXPERIMENTAL FACILITY AND INSTRUMENTATION

Test Facility

The Institute for Thermal Turbomachinery and Machine Dynamics at Graz University of Technology operates a 3MW compressor station in order to supply a couple of test facilities continuously with pressurized air. In the described subsonic turbine test facility the maximum pressure ratio is limited to 2 due to the inlet spiral casing. The maximum mass flow rate is 15 kg/s at a temperature at stage inlet of 100 °C. This inlet temperature can be adjusted by coolers within a wide range. The pressurized air enters the facility through a spiral inlet casing where the flow turns into axial direction. Within this spiral inlet casing the front bearing of the overhung-type turbine shaft is mounted. The shaft is coupled to a water brake, whose cooling water cycle is connected to the re-cooling plant of the institute.

In order to provide well defined and uniform inflow conditions a de-swirler together with a perforated plate is located upstream of the stage inlet. Furthermore, upstream of the stage (and downstream of the perforated plate) inlet guide vanes can be found that should simulate additional wakes of other upstream low pressure turbine stages. The air leaves the rig through an acoustic measurement section, supporting struts, exhaust casing, and the exhaust stack to ambient. A detailed description of the subsonic test turbine facility for aerodynamic, acoustic, and aeroelastic investigations (STTF-AAAI) is given in (Moser, et al., 2007).

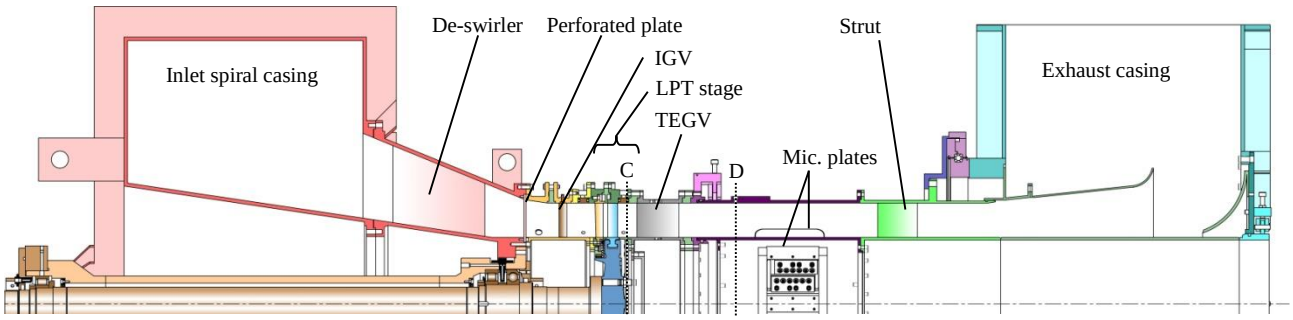

Figure 1: Meridional section of the STTF-AAAI

Turbine Stage and TEGVs

The aerodynamic design of the low pressure turbine stage, inlet guide vanes as well as the TEGVs was performed by MTU Aero Engines. Considerable effort was put into the adjustment of relevant model parameters to reproduce the full scale LPT configuration. The turbine diameter is approximately half that of a commercial aero engine LPT and therefore the rig is operated at higher rotational speeds. A meridional section of the rig is shown in Figure 1. The bladings are not drawn to scale. The rig is characterised by a high aspect ratio unshrouded rotor followed by the TEGVs of the TEC. Relevant geometry parameters can be seen in the upper half of Table 1.

For this investigation two different set-ups have been tested. A state-of-the-art TEC that is referred to as the reference TEC and a TEC with additive manufactured turbine exit guide vanes with Helmholtz resonators. The aerodynamic design is the same for both TEGVs.

Table 1: Geometry details and operating conditions

Geometry details	
Number of blades/vanes	
IGV/Stator/Rotor/	83/96/72
TEGV state-of-the-art (Reference TEC)	15
TEGV resonator	15
Tip gap to blade height ratio	1.0%
Hub to tip radius ratio	≈2/3
Operating conditions	
TEGV Reynolds number	~340000
Diffusion factor.	~0.5
Stage pressure ratio (approach)	1.16
Corrected speed (approach)	4042 rpm
Reduced mass flow rate (approach)	6.94 kg/s
Stage total inlet temperature	100 °C

Figure 2 shows the suction side of a single vane of the resonator TEC on the left side and a section of the whole TEC on the right side. In order to achieve a broadband effectiveness, the TEGV was equipped with four different resonators. Three separated volumes in radial direction and an additional volume at midspan. Each resonator consists of three rows of holes (each row has 20 holes) on the suction side which connect the volumes with the flow channel. The middle row of mentioned holes is located at 15% axial chord length concerning the three radial volumes. The second midspan volume is located a little bit further downstream at 35% axial chord length. The geometrical details of the resonators are given in Table 2.

Table 2: Resonator TEGV details

No. of holes per Volume	60
Hole diameter	0.9 mm
Neck length	1.2 mm
Volume size	Hub:1300 mm³/ Mid span:1345 mm³ and 1341 mm³/ Tip:1450 mm³
End correction (form factor)	0.352 mm

The value of the end correction δ_{tot} was experimentally determined and is about 1/4 of that calculated according the equation given in (Alster, 1972). It was necessary to measure the end correction factor due to the simple fact that the shape of the inlet and outlet of the neck is not known because of the additive manufacturing of the TEGVs and that the shape of the volumes differ from that given in classical literature. E.g. (Alster, 1972) mentioned that the shape of the volume has some influence on the resonant frequency of the Helmholtz resonator even the shape does not appear in the classical formula (see equation (1)).

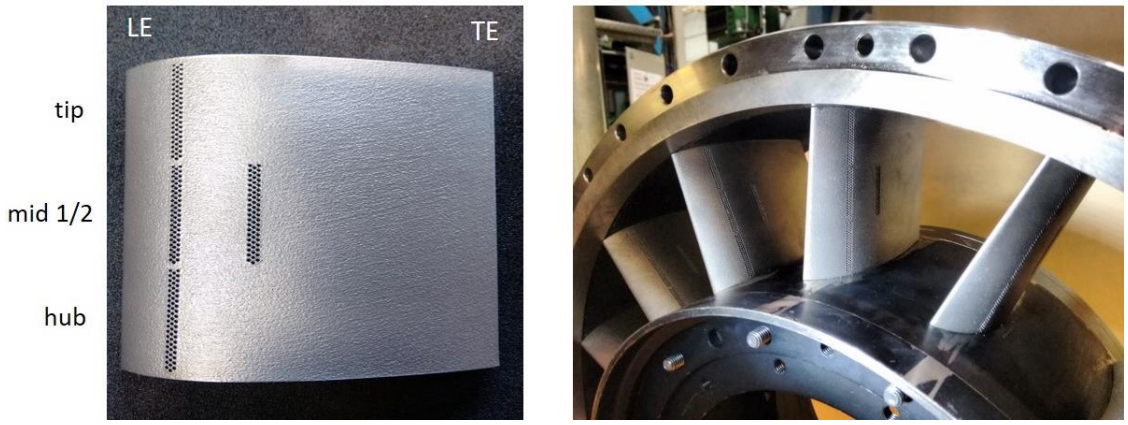

Figure 2: Helmholtz resonator TEGV

The classical formula of designing a resonator is given in equation (1).

$$f_{res} = \frac{c}{2\pi}\sqrt{\frac{S}{V(l+\delta_{tot})}} \tag{1}$$

With this formula and the geometrical dimensions of Table 2 the frequencies for the single resonators are calculated and presented in Table 3. The speed of sound at the investigated operation point approach is constantly 378 m/s.

Table 3: Design frequencies

f_hub	f_mid1	f_mid2	f_tip
8292.7 Hz	8152.8 Hz	8164.9 Hz	7852.1 Hz

Operating Conditions

Based on the intended use of the LPT rig for aeroelastic, acoustic and aerodynamic investigations, the main operating points are selected according to the typical noise certification points. They have been defined using an aero design point of the last stage LPT, derived from current LPT design practice using scaling along reduced speed, reduced mass flow (both referred to 288.15 K and 1013.25 mbar) and pressure ratio. For this investigation the operating point approach is chosen. The Reynolds number of the EGVs is defined using the midspan conditions at rotor exit as well as the axial chord of the vanes. The lower half of Table 1 shows the operating conditions.

Instrumentation

In order to estimate the sound power propagating downstream 12 flush mounted condenser microphones (1/4") at the hub and 12 at the casing are located in the 360 degrees rotatable acoustic measurement section. In addition to these microphones 1 microphone was mounted at a fixed position downstream of the TEGV's trailing edge as a reference. The complete sound field was detected at the hub and the casing by traversing the section 360 degrees in steps of 2 degrees. Some more detailed information about the acoustic measurement section is given in (Moser, et al., 2009).

Measurement Uncertainty

Instrumentation has to meet not only high demands on accuracy and repeatability but requires higher numbers of channels, too. Therefore, the measurement system is made up by eleven multi channel pressure transducers PSI 9016 with a total amount of 176 channels and an accuracy of 0.05% full scale and four National Instruments Field Point FP-TC-120 eight-channel thermocouple input

modules and one FP-RTD-122 resistance thermometer input module. Table 4 shows the measurement uncertainties (within a 95% confidence interval) of the five-hole-probe measurements. These values are positive and negative deviations and contain the error due to the approximation, random error and the systematic error of the PSI Modules. The difference between the positive and the negative direction is a result of the multi-parameter approximation. The measurement uncertainties of the static pressure and the total pressure at rig and stage inlet are +/- 1 mbar. Total pressure measurements up- and downstream of the TEGVs have an uncertainty of +/- 1 mbar.

Table 4 Measurement uncertainties of the five-hole-probe

Ma	+0.006	-0.003	[/]
α	+0.5	-0.08	[deg]
p_t	+3.3	-3.0	[mbar]
p	+5.3	-5.2	[mbar]

An estimation of the overall uncertainty of the total pressure loss coefficient ζ gives a value of +/- 0.0014. The variation of speed is below 0.2% of the current operating speed and the measurement uncertainty of the temperature measurement is about +/- 0.5 K. The variation of the operating parameters (pressure ratio, corrected speed, speed, total pressure and temperature at rig inlet) between different measurement days has been below 0.5%.
Measurement errors of the microphones (sound pressure measurement) are within 1 dB.

Acoustic Measurements and Mode Analysis

A decomposition of a variable in time and space was provided by (Tyler & Sofrin, 1962). The circumferential (azimuthal) mode orders excited by the relevant airfoil interactions can be calculated as follows:

$$m = n \cdot B + k_1 \cdot V_1; \quad k_1 = -\infty, \dots, -1,0,1, \dots + \infty \tag{2}$$

With the vane and blade counts V_1 and B, respectively, the harmonic order n, and the integer index k as well as an additional similar equation describing the scattering of acoustic modes when interacting with a following vane. V_2 is again the blade count of the vane.

$$m_S = m + k_2 \cdot V_2; \quad k_2 = -\infty, \dots, -1,0,1, \dots + \infty \tag{3}$$

In order to describe the sound generating mechanisms, Tyler and Sofrin wrote the pressure fluctuations at any circumferential position downstream of the compressor stage as a sum of harmonics. The theoretical model they proposed has been verified by numerous aeroacoustic experimental investigations and it is also valid for turbines (e.g. (Moser, et al., 2009)). The theory of acoustic data analysis used in this work is well described in (Enghardt, et al., 2001) and (Enghardt, et al., 2005). In cylindrical coordinates and for a single frequency component ω the solution of the wave equation is given by a linear superposition of modal terms as can be seen in equation (4).

$$p(x, r, \varphi, t) = \sum_{m=-\infty}^{\infty} \sum_{n=0}^{\infty} \left(A_{mn}^{\pm} e^{ik_{mn}^{\pm} x} \right) f_{mn} e^{im\varphi} e^{-i\omega t} \tag{4}$$

Herein the factor $k_{mn}^{\pm} = \frac{\tilde{\mathrm{k}}}{1-\mathrm{Ma}_{\mathrm{ax}}^2}[-\mathrm{Ma}_{\mathrm{ax}}^2 \pm \alpha_{\mathrm{mn}}]$ are the axial wave number upstream (-) and downstream (+), respectively. $\tilde{\mathrm{k}} = \frac{\omega}{c} - m\frac{\Omega}{c}$ is a modification of the wave number definition (Morfey, 1971).

For hard-walled acoustic boundary conditions the modal shape factor is reported in (Tapken & Enghardt, 2006). They also describe the calculation of complex mode amplitudes $A_{mn}^{\pm}$as an inverse problem of the equation (4), which is also applied in this work.

The sound power is computed according to equation (5) (Morfey, 1971) and involves only cut-on modes of the investigated system.

$$\mathrm{P}_{\mathrm{mn}}^{\pm} = \frac{\pi \mathrm{R}^2}{\rho c}\frac{\alpha_{\mathrm{mn}}(1-\mathrm{Ma}_{\mathrm{ax}}^2)^2}{(1 \mp \alpha_{\mathrm{mn}}\mathrm{Ma}_{\mathrm{ax}})^2}|\mathrm{A}_{\mathrm{mn}}^{\pm}|^2 \tag{5}$$

The factor $\alpha_{\mathrm{mn}} = \sqrt{1-(1-\mathrm{Ma}_{\mathrm{ax}}^2)\frac{\sigma_{\mathrm{mn}}^2}{(\tilde{\mathrm{k}}\mathrm{R})^2}}$ contains the definition of the cut-on frequency. If the m mode is to high the expression under the square root gets negative. This results in an imaginary factor α_{mn} which means that the sound wave can't propagate anymore and is therefore cut-off.

Cut-Off Modes

If $k_{mn}^{\pm}$ is real the (m, n) mode propagates energy and is therefore cut-on. The associated frequency is given by:

$$f_c = \frac{\sigma_{mn}}{2\pi R}c\sqrt{1-\mathrm{Ma}_{\mathrm{ax}}^2} \tag{6}$$

For a certain Mach number and frequency only a limited number of azimuthal modes can propagate. The highest mode order m at operating point approach for the first blade passing frequency (1BPF) is +/-19 and for the frequency of interest +/-30. All other modes are predicted to be cut-off.

RESULTS AND DISCUSSION

Acoustic Results

Figure 3 shows the frequency spectra (average of all microphones) of the sound pressure level (SPL) for the reference case on the left side and the resonator case on the right side.

The frequency of interest (FoI) is chosen as an arbitrary non-synchronous frequency in the spectrum. In the present work this frequency is attributed to a vibrating structure which is described in (Schönleitner, et al., 2015). The resonator is designed to reduce the peak of this specific frequency. It is assumed that every frequency can be removed from the spectra if it is possible to remove this one.

It can be seen that the sound pressure level (mainly flow noise) is reduced significantly due to the modifications of the EGVs. In Figure 3 on the left side the sound pressure level of the resonator case is depicted as dashed line. A reduction of ~9 dB is achieved at the FoI. At the first and second BPF a reduction of 8 and 9 dB can be seen, respectively. It is assumed that a change in boundary layer state on the suction side is responsible for this reduction. A first suggestion is, that the holes of the resonator vanes force the boundary layer to be turbulent, thus reducing boundary layer thickness and therefore the profile thickness noise is reduced. (van Nesselrooij, et al., 2016) showed that a dimpled surface can reduce drag but a high density pattern (as it is on the surface of the SS of the TEGV) increases the drag.

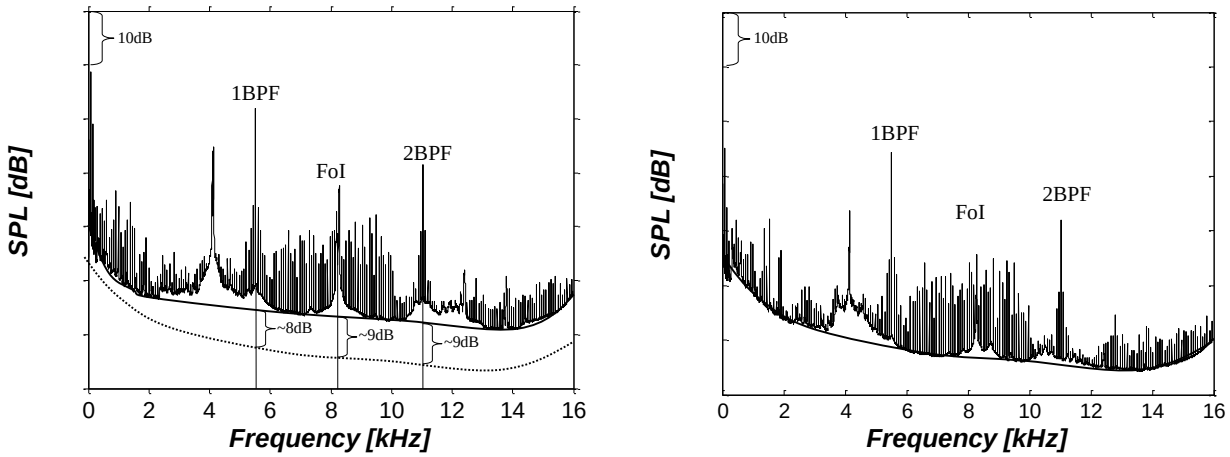

Figure 3: Frequency spectra; reference TEC (left) and resonator TEC (right)

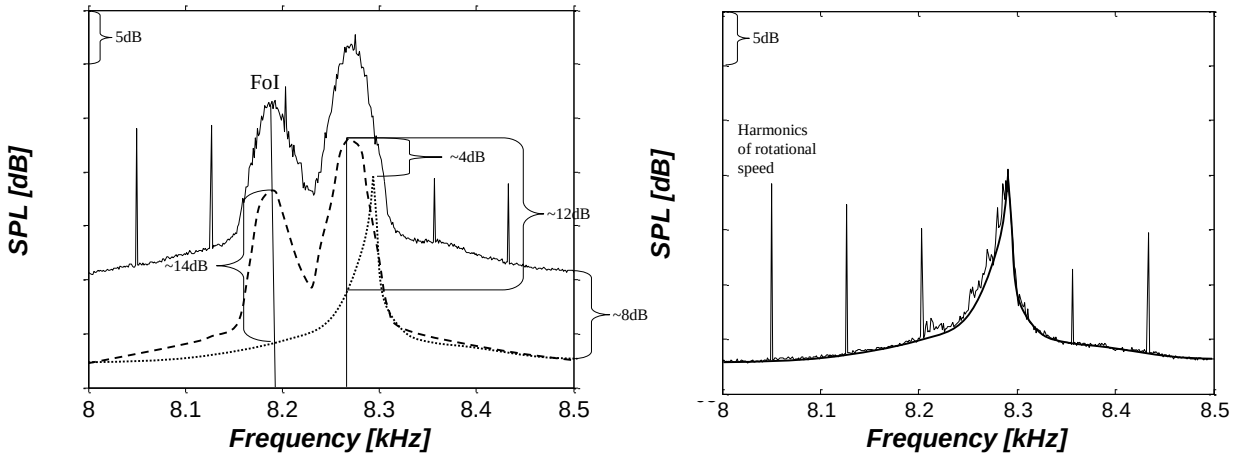

Figure 4: Frequency spectra (band width 0.5 kHz); reference TEC (left) and resonator TEC (right)

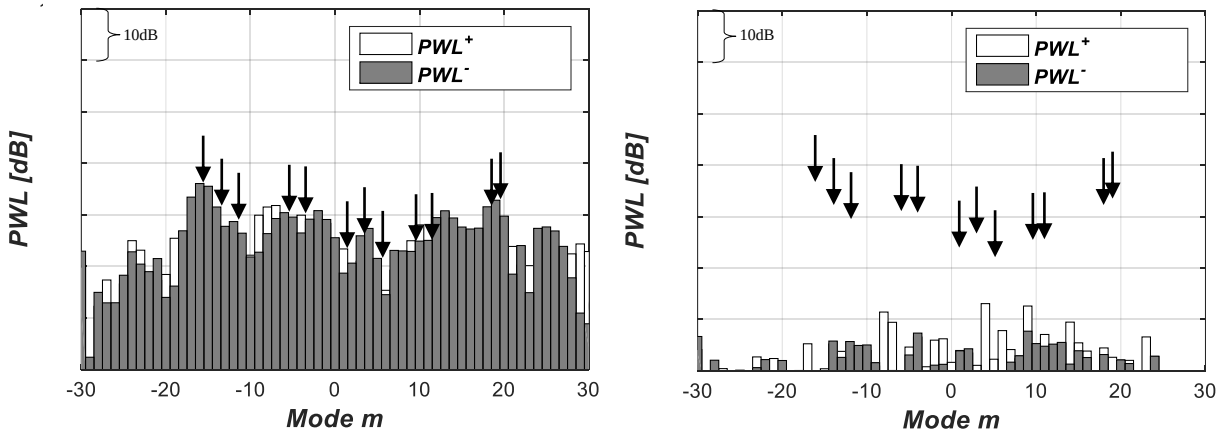

Figure 5: Modal sound power level for 8189 Hz (FoI); reference TEC (left) and resonator TEC (right)

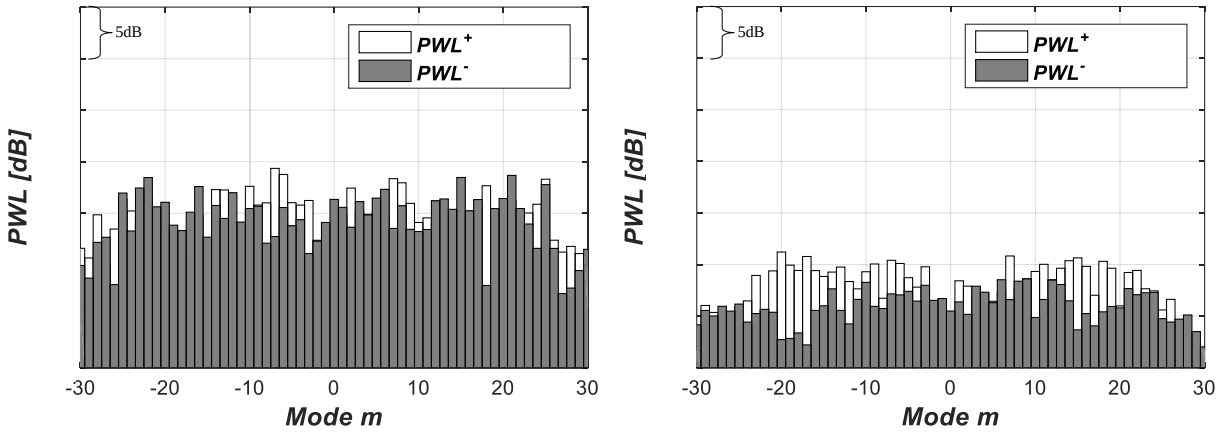

Figure 6: Modal sound power level for 8270 Hz; reference TEC (left) and resonator TEC (right)

In Figure 4 the frequency spectra are plotted in a zoom of the frequency range between 8 kHz and 8.5 kHz. On the left the spectrum of the reference TEC and on the right the spectrum of the resonator TEC can be seen. Additionally, in the left figure a dotted line representing the envelope of the resonator TEC spectrum without the harmonics of the rotational speed is drawn. The dashed line in the left figure represents the envelope of the reference TEC spectrum shifted by the amount of flow noise reduction.

This plot shows that the FoI is completely removed from the spectrum. Subtracting the amount of flow noise reduction (~8 dB) a reduction of 14 dB due to the Helmholtz resonator can be identified. Also the other peak at a frequency of about 8.3 kHz has also disappeared (reduced by app. 12 dB). The neighbouring peak is reduced by 4 dB as well.

Figure 5 and Figure 6 show the modal sound power level at a frequency of 8189 Hz (FoI) and 8270 Hz. The black arrows indicate the airfoil interaction modes given in Table 5. The arrows in the right figure are at the same level than in the left one. In Figure 5 on the left side the interaction modes can be seen. In the right figure it can be seen that all modes are reduced significantly. It can also be noticed that some of the interaction modes are lower than 30 dB.

In Table 6 and Table 7 the sound power level reduction of the amplitudes in and against flow direction, as well as the overall reduction is given. Reductions of 20 dB and 14 dB can be achieved due to the resonator, respectively.

Table 5 Airfoil interaction modes

Configuration	IGV-Rotor	Vane-Rotor	Rotor-TEC
Reference TEC	-4, +11, -19	-6, +9	-16, -14, -12, +1, +3, +5, +18
Resonator TEC	-4, +11, -19	-6, +9	-16, -14, -12, +1, +3, +5, +18

Table 6 Overall sound power level change for 8189 Hz (FoI)

	$\sum PWL^{+}$	$\sum PWL^{-}$	$\sum PWL^{\pm}$
Reference TEC	0.0 [dB]	0.0 [dB]	0.0 [dB]
Resonator TEC	-20.3 [dB]	-25.8 [dB]	-23.1 [dB]

Table 7 Overall sound power level change for 8270 Hz

	$\sum PWL^{+}$	$\sum PWL^{-}$	$\sum PWL^{\pm}$
Reference TEC	0.0 [dB]	0.0 [dB]	0.0 [dB]
Resonator TEC	-14.0 [dB]	-18.0 [dB]	-15.4[dB]

TEGV Inlet Flow: Plane C

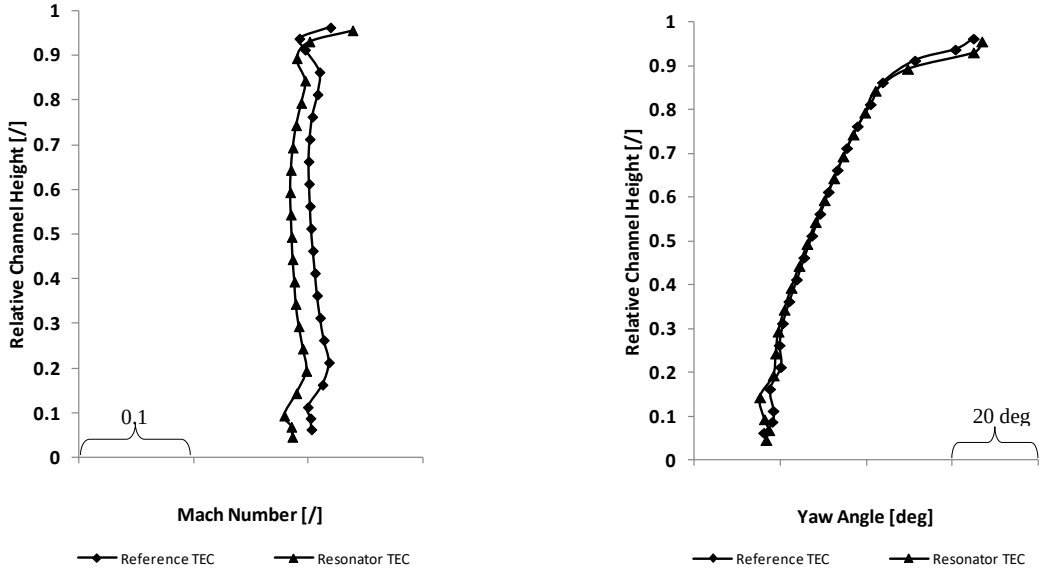

Figure 7: Mach number distribution (left) and yaw angle distribution (right) at TEC inlet

In Figure 7 the mass averaged Mach number distribution (left) and yaw angle distribution (right) at TEC inlet (plane C in Figure 1 marked as dotted line) are plotted. For both experiments the same inlet conditions have been realised. Figure 8 shows mass averaged Mach number and yaw angle distribution downstream of the TEC (plane D in Figure 1 marked as dotted line). The Mach number is the same for both set ups up to about 60% relative channel height. Above 60% the Mach number for the resonator TEC is a little bit smaller. The yaw angle distribution is completely different. At about 30% relative channel height a difference of 5 degrees can be seen between the set ups. The resonator TEC shows stronger over- and underturning than the reference TEC.

TEGV Outlet Flow: Plane D

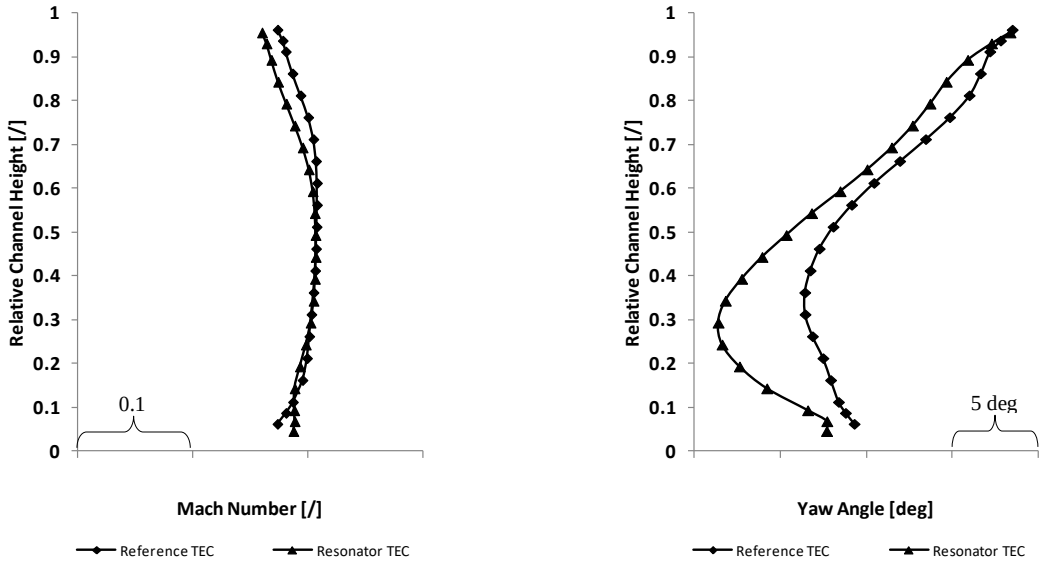

Figure 8: Mach number distribution (left) and yaw angle distribution (right) at TEC outlet

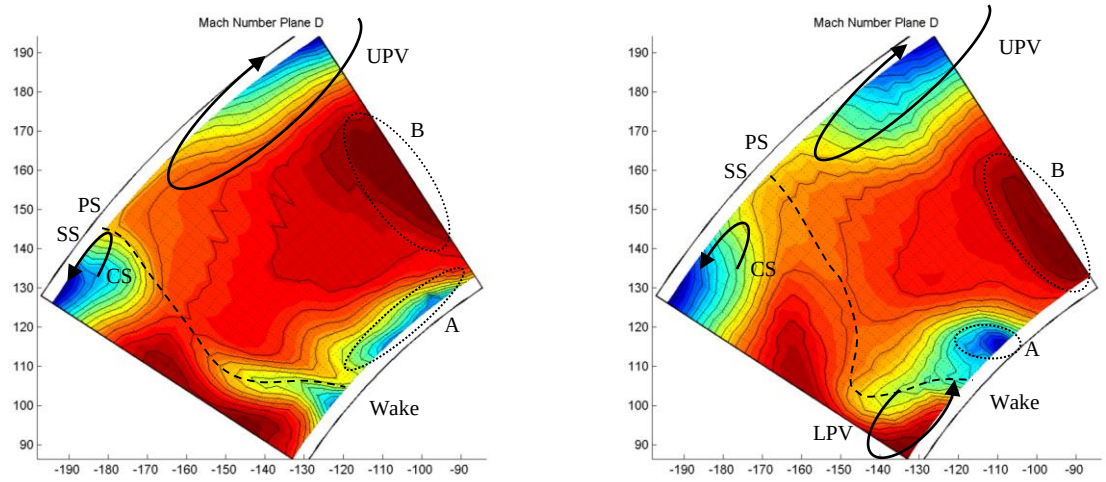

Figure 9: Mach number in plane D; reference TEC (left) and resonator TEC (right)

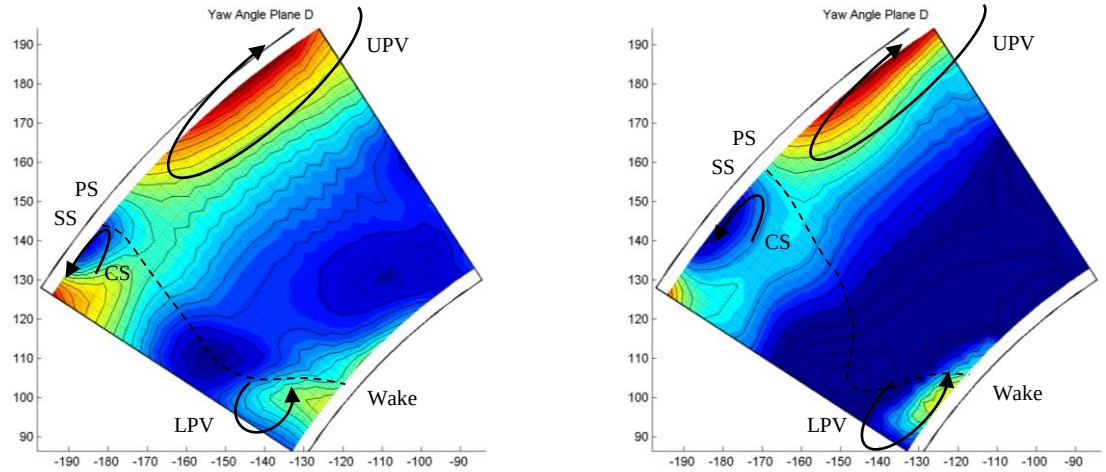

Figure 10: Yaw angle in plane D; reference TEC (left) and resonator TEC (right)

Figure 9 shows the Mach number downstream of the TEC in plane D and Figure 10 shows the yaw angle in the same measurement plane. Both figures are viewed from downstream. Red colour means a high Mach number or angle, blue a small one. The dashed lines in the figures represent the TEC wake. Below 30% relative channel height the wake for the resonator TEC is heavily skewed due to a stronger lower passage vortex (LPV). Also the upper passage vortex (UPV) seems to be stronger for the resonator TEC than for the reference TEC (comparing vorticity that is not depicted here). At the tip at the suction side of the wake a low Mach number region due to a corner separation (CS) can be identified. This region is larger for the resonator TEC than for the reference TEC. Further, below 70% relative passage height the yaw angle is more negative for the resonator TEC than for the reference TEC.

At the hub a low Mach number region (marked with A) can be identified, that is more concentrated at the pressure side of the wake for the resonator TEC. The high Mach number region (B) on the right side of the flow field is at lower radii for the resonator TEC.

The suction side was chosen as location for the holes because accordingly with CFD simulations this is where the biggest pressure fluctuations occur

Loss Estimation

Equation (7) gives a rough estimation of the total pressure loss coefficient from plane C upstream of the TEGVs to plane D downstream of the TEGVs. The total pressure has been mass averaged by means of the five-hole probe data.

$$\zeta = \frac{\overline{\overline{p}}_{t,C} - \overline{\overline{p}}_{t,D}}{\overline{\overline{p}}_{t,C} - p_{ex}} \tag{7}$$

Comparing the pressure loss coefficient of the reference TEC ζ_{ref} and the resonator TEC ζ_{res} reveals that the resonator TEC produces a twice higher total pressure loss than the reference TEC.

CONCLUSIONS

In this work two turbine exit guide vane set ups have been tested. Aerodynamically, both set ups are identically but one was designed as Helmholtz resonator. The resonator is designed to reduce the frequency of interest at 8189 Hz. It is shown that a sound power level reduction of 23 dB can be achieved. In terms of noise reduction resonators have great potential to help to achieve the ACARE targets. It is shown that a resonator TEGV can be successfully applied and operated under engine realistic operating conditions. The big advantage of such a resonator is that it is free of movable parts and produces low maintenance costs and can be easily retrofitted in every engine. However, it is shown that the flowfield downstream of the TEC is altered resulting in significantly higher losses. That implies that there must be an additional aerodynamic optimisation including the cavity and holes of the resonators. Therefore, the demand for high fidelity computations is evident. Furthermore, there will be more tests concerning the boundary layer of the vanes.

ACKNOWLEDGEMENTS

The authors thank Dr.techn. H.P. Pirker for operating the compressor station and his great support and discussions during all experimental investigations. Also Ulf Tapken, Mirko Spitalny and Prof. Dr. Lars Enghardt from the German Aerospace Centre (DLR) Institute of Propulsion Technology, Engine Acoustic Department, are gratefully acknowledged for supporting the acoustic data evaluation.

Further, the EU project VITAL (AIP4-CT-2004-012271) is acknowledged in which 1 TEC configuration has been designed, manufactured and operated.

This work has been carried out in the framework of the national funded TAKE-OFF programme within the research project hallstaTt (contract no. 850444) regarding sound power reductions of low pressure turbine by means of modifications on the turbine exit guide vanes at Graz University of Technology at the Institute for Thermal Turbomachinery and Machine Dynamics. The authors therefore thank the Austrian Research Promotion Agency (FFG) and the Austrian Ministry for Transport, Innovation and Technology (bmvit) for funding this project.

REFERENCES

Broszat, D., Selic, T. & Marn, A., 2012. Verification of the Inverse Cut-Off Effect in a Turbomachinery Stage Part 1-Numerical Results. *18th AIAA/CEAS Aeroacoustic Conference*, 4-6 June, pp. 1-9.

Enghardt, L., Tapken, U., Kornow, O. & Kennepohl, F., 2005. Acoustic Mode Decomposition of Compressor Noise Under Consideration of Radial Flow Profiles. *11th AIAA/CEAS Aeroacoustic Conference*, pp. 1-13.

Enghardt, L. et al., 2001. Turbine Blade/Vane Interaction Noise: Acoustic Mode Analysis Using In-Duct Sensor Arrays. *7th AIAA/CEAS Aeroacoustic Conference*, 28-30 May, pp. 1-8.

Hjärne, J., 2007. *Turbine Outlet Guide Vane Flows.* Göteborg: Chalmers University of Technology.

Koch, H., Kozulovic, D. & Hoeger, M., 2012. Outlet Guide Vane Airfoil for Low Pressure Turbine Configurations. *42nd AIAA Fluid Dynamics Confernce*, 25-28 June, pp. 1-10.
Marn, A. et al., 2014. Comparison of the Aerodynamics of Acoustically Designed EGVs and a State-of-the-Art EGV. *Proceedings of ASME TurboExpo*.
Marn, A. et al., 2015. Comparison of the Sound Power Levels of an Aerodynamically Designed EGV and a State-of-the-Art EGV. *Proceedings of ASME TurboExpo*.
Marn, A. et al., 2016. Comparison of the Fraction of the Sound Power Level due to Rotor-TEC-Interaction with the Overall Sound Power Level for Different Turbine Exit Guide Vane Designs. *22nd AIAA/CEAS-Aeroacoustic Conference*.
Morfey, C., 1971. Sound Transmission and Generation in Ducts with Flow. *Journal of Sound and Vibration*, 14(1), pp. 37-55.
Moser, M., Kahl, G., Kulhanek, G. & Heitmeir, F., 2007. *Construction of a Subsonic Test Turbine Facility for Experimental Investigations of Sound Generation and Propagation for Low Pressure Turbines*, Beijing, China: s.n.
Moser, M., Tapken, U., Enghardt, L. & Neuhaus, L., 2009. An Investigation of Low Pressure Turbine Blade-Vane Interaction Noise: Measurements in a 1.5-Stage Rig. *Proceedings of the Institution of Mechanical Engineers, Part A: Journal of Power and Energy*, 223(6), pp. 687-695.
Schönleitner, F. et al., 2015. Experimental Blade Vibration Measurements on Rotating Turbomachinery. *20th Blade Mechanics Seminar*.
Sonoda, T. & Schreiber, H.-A., 2007. Aerodynamic Characteristics of Supercritical Outlet Guide Vanes at Low Reynolds Number Conditions. *ASME Journal of Turbomachinery*, Band 129, pp. 694-704.
Sonoda, T. et al., 2004. Advanced High Turning Compressor Airfoils for Low Reynolds Number Condition-Part I: Design and Optimization. *ASME Journal of Turbomachinery*, Band 126, pp. 350-359.
Tapken, U. & Enghardt, L., 2006. Optimization of Sensor Arrays for Radial Mode Analysis in Flow Ducts. *12th AIAA/CEAS Aeroacoustics Confernence*, pp. 1-20.
Tyler, J. & Sofrin, T., 1962. Axial Flow Compressor Noise Studies. *SAE Transactions*, Band 70, pp. 309-332.
van Nesselrooij, M., Veldhuis, L., van Oudheusden, B. & Schrijer, F., 2016. Drag Reduction by Means of Dimpled Surfaces in Turbulent Boundary Layers. *Experiments in Fluids*, 142(57), pp. 11-14.